EUROPEAN ORGANISATION FOR NUCLEAR RESEARCH

CERN-PPE/90-189
18 December 1990

Measurement of the Cross Sections of the Reactions $e^+e^- \to \gamma\gamma$ and $e^+e^- \to \gamma\gamma\gamma$ at LEP

The OPAL Collaboration

Abstract

The cross section of the pure QED process $e^+e^- \to \gamma\gamma$ has been measured using data accumulated during the 1989 and 1990 scans of the Z^0 resonance at LEP. Both the energy dependence and the angular distribution are in good agreement with the QED prediction. Upper limits on the branching ratios of $Z^0 \to \gamma\gamma$, $Z^0 \to \pi^0\gamma$ and $Z^0 \to \eta\gamma$ have been set at 1.4×10^{-4}, 1.4×10^{-4} and 2.0×10^{-4} respectively. Lower limits on the cutoff parameters of the modified electron propagator have been found to be $\Lambda_+ > 117$ GeV and $\Lambda_- > 110$ GeV. The reaction $e^+e^- \to \gamma\gamma\gamma$ has also been studied and was found to be consistent with the QED prediction. An upper limit on the branching ratio of $Z^0 \to \gamma\gamma\gamma$ has been set at 6.6×10^{-5}. All the limits are given at 95% confidence level.

(Submitted to Physics Letters B)

The OPAL Collaboration

M.Z. Akrawy[12], G. Alexander[22], J. Allison[15], P.P. Allport[5], K.J. Anderson[9], J.C. Armitage[6], G.T.J. Arnison[19], P. Ashton[15], G. Azuelos[17,d], J.T.M. Baines[15], A.H. Ball[16], J. Banks[15], G.J. Barker[12], R.J. Barlow[15], J.R. Batley[5], G. Beaudoin[17], A. Beck[22], J. Becker[10], T. Behnke[8], K.W. Bell[19], G. Bella[22], S. Bethke[11], O. Biebel[3], U. Binder[10], I.J. Bloodworth[1], P. Bock[11], H. Breuker[8], R.M. Brown[19], R. Brun[8], A. Buijs[8], H.J. Burckhart[8], P. Capiluppi[2], R.K. Carnegie[6], A.A. Carter[12], J.R. Carter[5], C.Y. Chang[16], D.G. Charlton[8], J.T.M. Chrin[15], P.E.L. Clarke[21], I. Cohen[22], W.J. Collins[5], J.E. Conboy[14], M. Couch[1], M. Coupland[13], M. Cuffiani[2], S. Dado[21], G.M. Dallavalle[2], S. De Jong[8], P. Debu[20], M.M. Deninno[2], A. Dieckmann[11], M. Dittmar[4], M.S. Dixit[7], E. Duchovni[25], I.P. Duerdoth[15], D.J.P. Dumas[6], P.A. Elcombe[5], P.G. Estabrooks[6], E. Etzion[22], F. Fabbri[2], P. Farthouat[20], H.M. Fischer[3], D.G. Fong[16], M.T. French[19], C. Fukunaga[23], A. Gaidot[20], O. Ganel[25], J.W. Gary[11], J. Gascon[17], N.I. Geddes[19], C.N.P. Gee[19], C. Geich-Gimbel[3], S.W. Gensler[9], F.X. Gentit[20], G. Giacomelli[2], V. Gibson[5], W.R. Gibson[12], J.D. Gillies[19], J. Goldberg[21], M.J. Goodrick[5], W. Gorn[4], D. Granite[21], E. Gross[25], J. Grunhaus[22], H. Hagedorn[10], J. Hagemann[8], M. Hansroul[8], C.K. Hargrove[7], I. Harrus[21], J. Hart[5], P.M. Hattersley[1], M. Hauschild[8], C.M. Hawkes[8], E. Heflin[4], R.J. Hemingway[6], R.D. Heuer[8], J.C. Hill[5], S.J. Hillier[1], D.A. Hinshaw[17], C. Ho[4], J.D. Hobbs[9], P.R. Hobson[24], D. Hochman[25], B. Holl[8], R.J. Homer[1], S.R. Hou[16], C.P. Howarth[14], R.E. Hughes-Jones[15], R. Humbert[10], P. Igo-Kemenes[11], H. Ihssen[11], D.C. Imrie[24], L. Janissen[6], A. Jawahery[16], P.W. Jeffreys[19], H. Jeremie[17], M. Jimack[8], M. Jobes[1], R.W.L. Jones[12], P. Jovanovic[1], D. Karlen[6], K. Kawagoe[23], T. Kawamoto[23], R.G. Kellogg[16], B.W. Kennedy[14], C. Kleinwort[8], D.E. Klem[18], G. Knop[3], T. Kobayashi[23], T.P. Kokott[3], L. Köpke[8], R. Kowalewski[6], H. Kreutzmann[3], J. Kroll[9], M. Kuwano[23], P. Kyberd[12], G.D. Lafferty[15], F. Lamarche[17], W.J. Larson[4], J.G. Layter[4], P. Le Du[20], P. Leblanc[17], A.M. Lee[16], M.H. Lehto[14], D. Lellouch[8], P. Lennert[11], C. Leroy[17], L. Lessard[17], S. Levegrün[3], L. Levinson[25], S.L. Lloyd[12], F.K. Loebinger[15], J.M. Lorah[16], B. Lorazo[17], M.J. Losty[7], J. Ludwig[10], J. Ma[4,b], A.A. Macbeth[15], M. Mannelli[8], S. Marcellini[2], G. Maringer[3], A.J. Martin[12], J.P. Martin[17], T. Mashimo[23], P. Mättig[3], U. Maur[3], T.J. McMahon[1], J.R. McNutt[24], F. Meijers[8], D. Menszner[11], F.S. Merritt[9], H. Mes[7], A. Michelini[8], R.P. Middleton[19], G. Mikenberg[25], J. Mildenberger[6], D.J. Miller[14], C. Milstene[22], M. Minowa[23], W. Mohr[10], C. Moisan[17], A. Montanari[2], T. Mori[23], M.W. Moss[15], P.G. Murphy[15], W.J. Murray[5], B. Nellen[3], H.H. Nguyen[9], M. Nozaki[23], A.J.P. O'Dowd[15], S.W. O'Neale[8,c], B.P. O'Neill[4], F.G. Oakham[7], F. Odorici[2], M. Ogg[6], H. Oh[4], M.J. Oreglia[9], S. Orito[23], J.P. Pansart[20], G.N. Patrick[19], S.J. Pawley[15], P. Pfister[10], J.E. Pilcher[9], J.L. Pinfold[25], D.E. Plane[8], B. Poli[2], A. Pouladdej[6], E. Prebys[8], T.W. Pritchard[12], H. Przysiezniak[17], G. Quast[8], M.W. Redmond[9], D.L. Rees[1], M. Regimbald[17], K. Riles[4], C.M. Roach[5], S.A. Robins[12], A. Rollnik[3], J.M. Roney[9], S. Rossberg[10], A.M. Rossi[2,a], P. Routenburg[6], K. Runge[10], O. Runolfsson[8], S. Sanghera[6], R.A. Sansum[19], M. Sasaki[23], B.J. Saunders[19], A.D. Schaile[10], O. Schaile[10], W. Schappert[6], P. Scharff-Hansen[8], S. Schreiber[3], J. Schwarz[10], A. Shapira[25], B.C. Shen[4], P. Sherwood[14], A. Simon[3], P. Singh[12], G.P. Siroli[2], A. Skuja[16], A.M. Smith[8], T.J. Smith[8], G.A. Snow[16], R.W. Springer[16], M. Sproston[19], K. Stephens[15], H.E. Stier[10], R. Stroehmer[11], D. Strom[9], H. Takeda[23], T. Takeshita[23], P. Taras[17], N.J. Thackray[1], T. Tsukamoto[23], M.F. Turner[5], G. Tysarczyk-Niemeyer[11], D. Van den plas[17], R. Van Kooten[8], G.J. VanDalen[4], G. Vasseur[20],

C.J. Virtue[18], H. von der Schmitt[11], J. von Krogh[11], A. Wagner[11], C. Wahl[10], J.P. Walker[1], C.P. Ward[5], D.R. Ward[5], P.M. Watkins[1], A.T. Watson[1], N.K. Watson[1], M. Weber[11], S. Weisz[8], P.S. Wells[8], N. Wermes[11], M. Weymann[8], G.W. Wilson[20], J.A. Wilson[1], I. Wingerter[8], V-H. Winterer[10], N.C. Wood[14], S. Wotton[8], T.R. Wyatt[15], R. Yaari[25], Y. Yang[4,b], G. Yekutieli[25], T. Yoshida[23], W. Zeuner[8], G.T. Zorn[16].

[1]School of Physics and Space Research, University of Birmingham, Birmingham, B15 2TT, UK
[2]Dipartimento di Fisica dell' Università di Bologna and INFN, Bologna, 40126, Italy
[3]Physikalisches Institut, Universität Bonn, D-5300 Bonn 1, FRG
[4]Department of Physics, University of California, Riverside, CA 92521 USA
[5]Cavendish Laboratory, Cambridge, CB3 0HE, UK
[6]Carleton University, Dept of Physics, Colonel By Drive, Ottawa, Ontario K1S 5B6, Canada
[7]Centre for Research in Particle Physics, Carleton University, Ottawa, Ontario K1S 5B6, Canada
[8]CERN, European Organisation for Particle Physics, 1211 Geneva 23, Switzerland
[9]Enrico Fermi Institute and Department of Physics, University of Chicago, Chicago Illinois 60637, USA
[10]Fakultät für Physik, Albert Ludwigs Universität, D-7800 Freiburg, FRG
[11]Physikalisches Institut, Universität Heidelberg, Heidelberg, FRG
[12]Queen Mary and Westfield College, University of London, London, E1 4NS, UK
[13]Birkbeck College, London, WC1E 7HV, UK
[14]University College London, London, WC1E 6BT, UK
[15]Department of Physics, Schuster Laboratory, The University, Manchester, M13 9PL, UK
[16]Department of Physics and Astronomy, University of Maryland, College Park, Maryland 20742, USA
[17]Laboratoire de Physique Nucléaire, Université de Montréal, Montréal, Quebec, H3C 3J7, Canada
[18]National Research Council of Canada, Herzberg Institute of Astrophysics, Ottawa, Ontario K1A 0R6, Canada
[19]Rutherford Appleton Laboratory, Chilton, Didcot, Oxfordshire, OX11 0QX, UK
[20]DPhPE, CEN Saclay, F-91191 Gif-sur-Yvette, France
[21]Department of Physics, Technion-Israel Institute of Technology, Haifa 32000, Israel
[22]Department of Physics and Astronomy, Tel Aviv University, Tel Aviv 69978, Israel
[23]International Centre for Elementary Particle Physics and Dept of Physics, University of Tokyo, Tokyo 113, and Kobe University, Kobe 657, Japan
[24]Brunel University, Uxbridge, Middlesex, UB8 3PH UK
[25]Nuclear Physics Department, Weizmann Institute of Science, Rehovot, 76100, Israel

[a]Present address: Dipartimento di Fisica, Università della Calabria and INFN, 87036 Rende, Italy
[b]On leave from Harbin Institute of Technology, Harbin, China
[c]On leave from Birmingham University
[d]and TRIUMF, Vancouver, Canada

The reaction $e^+e^- \rightarrow \gamma\gamma$ provides a clean test of QED at centre of mass energies near to the Z^0 resonance, in contrast to lepton pair production where the weak interaction is dominant. The study of this reaction can also be used to set limits on non-standard properties of the Z^0 boson. We have previously published a study of this reaction based on 21 $e^+e^- \rightarrow \gamma\gamma$ events [1], and similar results have been reported by other LEP collaborations [2,3,4]. In this paper we present an improved measurement of the cross section of this reaction using all the data accumulated by the OPAL experiment in 1989 and 1990 during scans in centre of mass energy across the Z^0 resonance. The integrated luminosity used is more than 10 times as large as that in our previous publication [1], which is superseded by this paper. The updated analysis of the higher order reaction $e^+e^- \rightarrow \gamma\gamma\gamma$ is also given.

The components of the OPAL detector [5] relevant to this analysis are described below. The trajectories and momenta of charged particles are measured by a central tracking detector in a uniform magnetic field of 0.435 T. It includes a precision vertex chamber, a large volume jet chamber which gives precise tracking information in the plane perpendicular to the beam direction and z-chambers for tracking in the plane parallel to the beam direction. The vertex chamber is a 1 metre long, 47 cm diameter cylindrical drift chamber. It consists of an inner layer of 36 cells with 12 axial wires per cell and an outer layer of 36 cells with 6 small angle (4°) stereo wires per cell. The main tracking is done with the jet chamber, a drift chamber approximately four metres long and two metres in radius. It provides up to 159 measured space points along a track and covers the polar angular range of $|\cos\theta| < 0.97$. The barrel part of the electromagnetic calorimeter covers the region $|\cos\theta| < 0.82$ and consists of 9440 lead glass blocks of 24.6 radiation lengths thickness pointing towards the interaction region. The blocks are slightly tilted from a perfect pointing geometry to prevent photons from escaping through inter-block gaps. The two endcaps of the electromagnetic calorimeter consist of 2264 lead glass blocks of 20 radiation lengths thickness, covering the polar angular range of $0.81 < |\cos\theta| < 0.98$. The energy resolution for a 45 GeV electron is typically 3% in the barrel and 4% in the endcaps although the energy resolution is degraded around the overlap region of the barrel and the endcaps. The forward detector, used for the luminosity measurement, is composed of two identical elements placed around the beam pipe at either end of the central detector, each consisting of a lead-scintillator calorimeter and proportional tube chambers. They cover the polar angles between 40 and 150 mrad and 2π in azimuthal angle. In front of each calorimeter there is a set of precisely located scintillators and drift chambers. The systematic normalisation error in the determination of the integrated luminosity is better than 1.6% [6].

For this analysis the vertex chamber, jet chamber, electromagnetic calorimeter and forward detector were all required to be operating at high efficiency. After these quality cuts, the remaining data correspond to an integrated luminosity of 7.21 pb^{-1}. The effective average centre of mass energy, calculated from the luminosity weighted mean value of $1/s$, is 91.22 GeV.

The triggers for $e^+e^- \rightarrow \gamma\gamma(\gamma)$ events are based on the electromagnetic calorimeter. The calorimeter trigger required an energy sum of at least 6 GeV in the barrel part or in one endcap. The trigger inefficiency for $e^+e^- \rightarrow \gamma\gamma(\gamma)$ events has been studied using $e^+e^- \rightarrow e^+e^-$ events, which had independent triggers, and was found to be negligible over the polar angular range considered.

The selection of $e^+e^- \rightarrow \gamma\gamma(\gamma)$ events was based on energy clusters in the electromagnetic calorimeters. Clusters in the barrel region were required to have an energy of at least 100 MeV and clusters in the endcaps were required to contain at least two adjacent lead glass blocks and have an energy of at least 200 MeV. Charged tracks in the central detector were used to identify photon conversions in $e^+e^- \rightarrow \gamma\gamma(\gamma)$ events and to separate them from events produced by background processes. Tracks used in this analysis were divided into two categories. One was a track reconstructed from the vertex chamber data only (vertex chamber track) and the other was a track reconstructed using the whole central detector, namely the vertex chamber, the jet chamber and the z-chambers (central detector track). A vertex chamber track could also be classified as a central detector track if it matched with a track which had been reconstructed in the jet chamber. A vertex chamber track had to have at least six wires hit, while the following quality requirements were imposed on central detector tracks.

- $|d_0| < 2$ cm, where $|d_0|$ is the distance of closest approach to the beam axis in a plane perpendicular to the beam axis.
- $|z_0| < 70$ cm, where $|z_0|$ is the distance of closest approach to the interaction point, along the beam axis.
- $N_{hit} \geq 20$, where N_{hit} is the total number of hits in the chambers associated with the track.
- The radius of the first hit from the beam axis had to be less than 60 cm.
- The momentum transverse to the beam axis had to be greater than 50 MeV/c.

The following event selection criteria were used to remove most of the backgrounds from Z^0 decays.

i) $N_{cls} \leq 8$, where N_{cls} is the number of electromagnetic clusters. This removed most of the multihadronic events.

ii) If there were two or more vertex chamber tracks, the maximum opening angle among the tracks in azimuth had to be less than 3°.

iii) If there were two or more central detector tracks, the maximum opening angle among the tracks had to be less than 20°.

Cuts ii) and iii) together removed most of the lepton pair events, as well as the multihadronic events.

The above cuts allowed one photon conversion per event in $e^+e^- \rightarrow \gamma\gamma(\gamma)$ events. Events with more than one photon conversion were not selected.

The final selection of $e^+e^- \rightarrow \gamma\gamma$ events was made by applying the following further cuts which required two high-energy, back-to-back photon clusters.

A1) At least two energetic electromagnetic clusters were required, each with an energy larger than 20% of the beam energy.

A2) The acollinearity angle of the two most energetic clusters was required to be less than 5°.

A3) $|\cos\theta|_{AV} < 0.9$, where θ is the polar angle and $|\cos\theta|_{AV}$ is the average $|\cos\theta|$ of the two clusters. (The geometrical acceptance was reduced from that used in our previous paper [1], $|\cos\theta| < 0.95$, in order to avoid a large uncertainty in the photon conversion probability in the forward region.)

A total of 205 events satisfied these criteria. All the events were scanned and it was confirmed that there remained no obvious background events due to track reconstruction inefficiency. The distributions of the second largest electromagnetic cluster energy and the acollinearity angle of the two most energetic clusters are compared with those of the Monte Carlo prediction for the reaction $e^+e^- \rightarrow \gamma\gamma$ in figures 1a and 1b respectively. The Monte Carlo events were generated by the RADCOR program [7] and processed by a program which simulates the response of the OPAL detector [8]. The agreement is good.

The remaining background from the process $e^+e^- \rightarrow e^+e^-(\gamma)$ was estimated using Monte Carlo simulations. The $e^+e^- \rightarrow e^+e^-\gamma$ events could fake the reaction $e^+e^- \rightarrow \gamma\gamma$ with one photon conversion in the following cases.

a) The electron and the positron were very close to each other and opposite to a high energy photon.

b) A photon and one of the electrons were emitted collinearly with most of the energy carried by the photon and the very low momentum charged track was not reconstructed in the chambers.

c) One of the electrons scattered at small angles and escaped detection and the other electron and a photon were back to back.

To estimate the backgrounds from the cases a) and b) we generated 24000 $e^+e^- \rightarrow e^+e^-(\gamma)$ events within the range $|\cos\theta| < 0.976$ at a centre of mass energy corresponding to the peak of the Z^0 resonance, using the BABAMC Monte Carlo program [9]. The number of events is equivalent to an integrated luminosity of 5.9 pb^{-1}. The events were processed by the detector simulation program [8] and the same selection criteria were applied to the simulated events as were applied to the real data. Only seven out of the 24000 generated events were found to be of the types a) or b) and the contribution to the cross section is 1.2 ± 0.5 pb at the Z^0 peak. The number of events expected for the total luminosity is 6.9 ± 2.6, where the $\sqrt{s}$ dependence of the $e^+e^- \rightarrow e^+e^-(\gamma)$ cross section has been taken into account. The case c) cannot be simulated by the BABAMC Monte Carlo program. Therefore this was simulated using the TEEGG Monte Carlo program [10]. The cross section and the number of background events were found to be 0.29 pb and 2.1 respectively. Other backgrounds from μ pairs, τ pairs [11] and multihadronic events [12] were also studied and were found to be negligibly small. The contribution from background events was subtracted from the selected events in the following analysis.

To study the selection efficiency of $e^+e^- \rightarrow \gamma\gamma$ events, 2793 events were generated in the angular region $|\cos\theta| < 0.98$ at the Z^0 peak energy by the RADCOR Monte Carlo program [7] and were then processed by the detector simulation program [8]. The number of simulated

events corresponds to an integrated luminosity of 44.6 pb^{-1}. The selection efficiency in the relevant angular region ($|\cos\theta|_{AV} < 0.9$) was found to be 99.5 ± 0.8 %. The systematic error is due to the geometrical uncertainty at $|\cos\theta| = 0.9$ and the finite angular resolution of electromagnetic clusters. The contributions are 0.7% and 0.4% respectively and were added in quadrature. The numbers of real events with at least one central detector track and with no central detector track were 28 and 177 respectively. Taking into account a total of 9.0 background events considered above, which would fake $e^+e^- \to \gamma\gamma$ events with one photon conversion, the 28 observed events are consistent with a conversion probability of 5.1 ± 1.4 %. The Monte Carlo simulation predicts this probability to be 4.3 ± 0.4 % in good agreement with the measurement.

Following the convention used for the analysis of lower energy e^+e^- data [13] we present our measurement as a lowest order cross section, after applying radiative corrections to account for higher order contributions. This produces a result which is independent of the choice of phase space cuts (except for the $|\cos\theta|$ cut) and which can therefore more easily be compared with the theoretical prediction and with measurements made by other experiments.

The integrated lowest order cross section, σ, was calculated using the following formula.

$$\sigma = \frac{(N_{obs} - N_{bg})}{\epsilon \mathcal{L} R}$$

where N_{obs}, N_{bg}, ϵ and $\mathcal{L}$ are the number of observed events, the number of background events, the selection efficiency and the integrated luminosity respectively. The parameter R is the ratio of the predicted cross section with radiative corrections complete to order α^3 to the predicted lowest order cross section. Using Monte Carlo calculations [7] we have evaluated R at $\sqrt{s} = 91.22$ GeV and with our selection criteria to be 0.844. We measure $\sigma = 32.4 \pm 2.3$ pb for $|\cos\theta| < 0.9$ at $\sqrt{s} = 91.22$ GeV. The QED prediction is 32.0 pb. The cross sections for $|\cos\theta| < 0.9$ for the different centre of mass energy points are given in table 1 and shown in figure 2a together with the QED prediction, which is proportional to $1/s$. The absolute value and the energy dependence of the cross section are in excellent agreement with QED. No significant influence from the Z^0 resonance on the reaction $e^+e^- \to \gamma\gamma$ is observed.

A possible deviation of the measured $e^+e^- \to \gamma\gamma$ cross section from the QED prediction could come from rare Z^0 decays such as $Z^0 \to \gamma\gamma$ (theoretically forbidden [14]) or $Z^0 \to \pi^0\gamma$ and $Z^0 \to \eta\gamma$ (the branching ratios are supposed to be of order 10^{-11} in the standard model [15]) in which the neutral decay of an energetic π^0 or η particle fakes a single high energy photon. The event topology of these Z^0 decays is similar to that of the QED reaction $e^+e^- \to \gamma\gamma$ except for the angular distribution, which is expected to be approximately proportional to $1 + \cos^2\theta$. The overall detection efficiencies were estimated to be 86%, 85% and 60% for the decays $Z^0 \to \gamma\gamma$, $Z^0 \to \pi^0\gamma$ and $Z^0 \to \eta\gamma$ respectively, where the geometrical acceptance, the conversion probability and the decay modes of the η have been taken into account. We have assumed that the cross section of $e^+e^- \to Z^0 \to X$ is given by a Breit-Wigner line shape with s-dependent width, convoluted with an initial state photon radiation function as described in [16]. There may be some interference between the QED processes and these rare Z^0 decays, but these effects were not taken into account in this analysis. The

peak cross section, $\sigma_{\rm peak}$, was expressed as

$$\sigma_{\rm peak} = \frac{12\pi}{M_{\rm Z}^2}\frac{\Gamma_{ee}\Gamma_X}{\Gamma_{\rm Z}^2}$$

where $M_{\rm Z}$ and $\Gamma_{\rm Z}$ are the mass and the total width of the Z^0 and Γ_{ee} and Γ_X are the partial decay widths of $Z^0 \to e^+e^-$ and $Z^0 \to X$. We defined a χ^2 function as

$$\chi^2(\Gamma_X, N_L) = \sum_i \left(\frac{\sigma_i - N_L\sigma_i(\Gamma_X)}{\Delta\sigma_i}\right)^2 + \left(\frac{1-N_L}{\Delta N_L}\right)^2$$

where σ_i and $\sigma_i(\Gamma_X)$ are the measured and the expected integrated cross sections for the centre of mass energy bin i. The normalisation factor, N_L, accounts for the systematic error of the luminosity measurement and was allowed to vary with the standard deviation $\Delta N_L = 1.6\%$. The contributions from QED and from $Z^0 \to X$ were summed in calculating $\sigma_i(\Gamma_X)$. Using this function with our measured values of $M_{\rm Z}$ (91.174 GeV), $\Gamma_{\rm Z}$ (2.505 GeV) and Γ_{ee} (83.6 MeV) [6], we determined upper limits on $\Gamma_{\gamma\gamma}$, $\Gamma_{\pi^0\gamma}$ and $\Gamma_{\eta\gamma}$ to be 0.36 MeV, 0.36 MeV and 0.51 MeV, respectively, at 95% confidence level. These limits correspond to $Br(Z^0 \to \gamma\gamma) < 1.4 \times 10^{-4}$, $Br(Z^0 \to \pi^0\gamma) < 1.4 \times 10^{-4}$ and $Br(Z^0 \to \eta\gamma) < 2.0 \times 10^{-4}$. These are compared with previous limits [1,2,3,4] in table 2.

The measured differential cross section for $e^+e^- \to \gamma\gamma$ is listed in table 3 and shown in figure 2b. The agreement between the data and the QED prediction is good. A deviation from QED can be parametrised by introducing cutoff parameters, $\Lambda_\pm$, into the electron propagator as follows [17].

$$\frac{d\sigma}{d\Omega} = \frac{\alpha^2}{s}\frac{1+\cos^2\theta}{1-\cos^2\theta}\left(1 \pm \frac{s^2}{2\Lambda_\pm^4}(1-\cos^2\theta)\right)$$

In order to obtain lower limits on $\Lambda_\pm$, a χ^2 function was defined as

$$\chi^2(\Lambda_\pm, N_L) = \sum_i \left(\frac{\frac{d\sigma}{d\Omega_i} - N_L\frac{d\sigma}{d\Omega_i}(\Lambda_\pm)}{\Delta\frac{d\sigma}{d\Omega_i}}\right)^2 + \left(\frac{1-N_L}{\Delta N_L}\right)^2$$

where $\frac{d\sigma}{d\Omega_i}$ and $\frac{d\sigma}{d\Omega_i}(\Lambda_\pm)$ are the measured and the expected differential cross sections for angular bin i, and N_L and ΔN_L have the same meanings as before. Using this function we obtained lower limits of $\Lambda_+ > 117$ GeV and $\Lambda_- > 110$ GeV at 95% confidence level. Our limits are compared with previous ones [1,2,3,4,13] in table 4.

The differential cross section for $e^+e^- \to \gamma\gamma$ can be modified by the exchange of a virtual excited electron, e^*, of mass M_{e^*} and with coupling constant λ, where the effective Lagrangian is written as [17]

$$L_{eff} = \frac{\lambda e}{2M_{e^*}}\bar{e}\sigma_{\mu\nu}e^*F^{\mu\nu} + h.c.$$

In the limit $M_{e^*}^2 \gg s$, the cutoff parameter Λ_+ is related to the excited electron mass by the equation $M_{e^*}^2/\lambda = \Lambda_+^2$. For this analysis $M_{e^*}^2 \approx s$ and so we have used the full formula given in the appendix of reference [17]. Assuming $\lambda = 1$, we obtained a lower limit on the mass of the excited electron of 116 GeV at 95% confidence level. This is consistent with previous limits [1,3] and with those obtained by direct searches for excited electrons at LEP [18].

Indirect searches using the reaction $e^+e^- \to \gamma\gamma$ are sensitive only to the electromagnetic coupling of an excited electron.

Events of the higher order QED process $e^+e^- \to \gamma\gamma\gamma$ were selected by replacing the criteria (A1 to A3) by (B1 to B3).

B1) Three energetic electromagnetic clusters were required, each with an energy larger than 10% of the beam energy and $|\cos\theta| < 0.9$. The sum of energies of other clusters had to be less than 2.5 GeV.

B2) The opening angles between any two energetic clusters had to be larger than 20°.

B3) The sum of the three opening angles had to be larger than 350°, to ensure that the event was planar.

The number of selected events was eight. Among these events only one event had one photon conversion. The number of events expected from QED was determined using a sample of 800 Monte Carlo $e^+e^- \to \gamma\gamma\gamma$ events which were generated in the angular region $|\cos\theta| < 0.95$ at the Z^0 peak energy by the RADCOR program [7] and then processed by the detector simulation program [8]. The number of simulated events corresponds to an integrated luminosity of 272 pb^{-1} and 204 events pass the above criteria. Thus the expected number of events for our integrated luminosity is $5.4 \pm 0.4 \pm 0.5$ where the first error is statistical and the second is systematic. Here we conservatively assumed a 10% systematic error because there is no exact calculation of radiative corrections for this process. The background from $e^+e^- \to e^+e^-\gamma\gamma$ events, in which one electron was emitted in the beam direction and escaped detection, was estimated to be 0.3 events by using the TEEGG program [10]. Backgrounds from μ pairs, τ pairs and multihadronic events are negligible. Therefore the observed number of events is consistent with the QED prediction. The numbers are listed in table 5 and the ratio of the observed number of events to the expected number of events is shown in figure 3a. Figure 3b shows the distribution of invariant masses of photon pairs, where the invariant mass is reconstructed from the opening angles between photons. This distribution also agrees well with the expectation.

A possible enhancement to the process $e^+e^- \to \gamma\gamma\gamma$ could come from the decay $Z^0 \to \gamma\gamma\gamma$. The branching ratio $Br(Z^0 \to \gamma\gamma\gamma)$ is 3×10^{-10} in the standard model [19], but it may be as large as 2×10^{-4} in some composite models [20,21]. The overall detection efficiency for the $Z^0 \to \gamma\gamma\gamma$ decay was estimated to be 69% by a Monte Carlo simulation, including the geometrical acceptance and the conversion probability. We assumed here an isotropic distribution of the event plane and the energy distribution of photons calculated for the $Z^0\gamma\gamma\gamma$ contact term [21]. Because of low statistics, the following likelihood function, L, was defined in order to obtain an upper limit on the decay width of $Z^0 \to \gamma\gamma\gamma$.

$$L(\Gamma_{\gamma\gamma\gamma}, N) = \frac{1}{\sqrt{2\pi}\Delta N} \exp\left(-\frac{1}{2}\left(\frac{1-N}{\Delta N}\right)^2\right) \prod_i P(N_i, \lambda_i(\Gamma_{\gamma\gamma\gamma}, N))$$

where P denotes the Poisson distribution function and N_i and λ_i are the observed and the expected numbers of events for centre of mass energy bin i. The factor, N, accounts for the normalisation errors, which are dominated by the systematic errors on the QED expectation,

and was allowed to vary with the standard deviation $\Delta N = 12.3\%$. In the calculation of λ_i, we assumed a pure QED process and a Breit-Wigner line shape for the $Z^0 \to \gamma\gamma\gamma$ decay, not taking their interference into account. Using this function we determined the upper limit on $\Gamma_{\gamma\gamma\gamma}$ to be 0.17 MeV at 95% confidence level, which corresponds to an upper limit of 6.6×10^{-5} on the branching ratio $Br(Z^0 \to \gamma\gamma\gamma)$. This is compared with previous limits [1,3] in table 2.

In summary, we have measured the total and differential cross section of the reaction $e^+e^- \to \gamma\gamma$ at centre of mass energies around the Z^0 resonance. Our measurement is in good agreement with the QED prediction. No influence of the Z^0 boson is observed and the upper limits on the branching ratios $Br(Z^0 \to \gamma\gamma)$, $Br(Z^0 \to \pi^0\gamma)$ and $Br(Z^0 \to \eta\gamma)$ were found to be 1.4×10^{-4}, 1.4×10^{-4} and 2.0×10^{-4} respectively. The lower limits on the cutoff parameters of the modified electron propagator are $\Lambda_+ > 117$ GeV and $\Lambda_- > 110$ GeV. Eight events from the higher order process $e^+e^- \to \gamma\gamma\gamma$ were observed, consistent with the QED prediction. The upper limit on the branching ratio $Br(Z^0 \to \gamma\gamma\gamma)$ was determined to be 6.6×10^{-5}. All the limits were obtained at 95% confidence level.

It is a pleasure to thank the SL Division for the efficient operation of the LEP accelerator and their continuing close cooperation with our experimental group. In addition to the support staff at our own institutions we are pleased to acknowledge the following :
Department of Energy, USA
National Science Foundation, USA
Science and Engineering Research Council, UK
Natural Sciences and Engineering Research Council,Canada
Israeli Ministry of Science
Minerva Gesellschaft
The Japanese Ministry of Education, Science and Culture (the Monbusho) and a grant under the Monbusho International Science Research Program.
American Israeli Bi-national Science Foundation.
Direction des Sciences de la Matière du Commissariat à l'Energie Atomique, France.
The Bundesministerium für Forschung und Technologie, FRG.
and The A.P. Sloan Foundation.

References

[1] OPAL collab., M. Z. Akrawy et al., Phys. Lett. B241 (1990) 133.

[2] ALEPH collab., D. Decamp et al., Phys. Lett. B241 (1990) 635.

[3] L3 collab., B. Adeva et al., Phys. Lett. B250 (1990) 199.

[4] DELPHI collab., P. Abreu et al., contribution to 25th International Conference on High Energy Physics, Singapore (August 1990), CERN-PPE/90-167 (November 1990).

[5] OPAL collab., K. Ahmet et al., "The OPAL Detector at LEP", CERN-PPE/90-114 (August 1990), to be published in Nucl. Instr. and Meth.

[6] OPAL collab., contribution by T. Mori to the 25th International Conference on High Energy Physics, Singapore (August 1990);
M. Z. Akrawy et al., Phys. Lett. B240 (1990) 497.

[7] F. A. Berends and R. Kleiss, Nucl. Phys. B186 (1981) 22.

[8] J. Allison et al., Computer Physics Communications 47 (1987) 55.

[9] M. Böhm, A. Denner and W. Hollik, Nucl. Phys. B304 (1988) 687;
F. A. Berends, R. Kleiss and W. Hollik, Nucl. Phys. B304(1988) 712.

[10] D. Karlen, Nucl. Phys. B289 (1987) 23.

[11] S. Jadach et al., Z Physics at LEP 1, CERN 89-08, ed. G.Altarelli et al., Vol. 1 (1989) 235;
KORALZ, Version 37.

[12] T. Sjöstrand, Comp. Phys. Comm. 39 (1986) 347;
G. Marchesini and B.R. Webber, Nucl. Phys. B310 (1988) 461.

[13] CELLO collab., H. -J. Behrend et al., Phys. Lett. 103B (1981) 148;
Phys. Lett. 123B (1983) 127; Phys. Lett. 168B (1986) 420;
JADE collab., W. Bartel et al., Phys. Lett. 92B (1980) 206; Z. Phys. C19 (1983) 197;
B. Naroska, Phys. Rep. 148 (1987) 67;
MARK J collab., B. Adeva et al., Phys. Rev. Lett. 53 (1984) 134;
Phys. Lett. 152B (1985) 439;
PLUTO collab., Ch. Berger et al., Phys. Lett. 94B (1980) 87;
TASSO collab., M. Althoff et al., Z. Phys. C 26 (1984) 337;
HRS collab., M. Derrick et al., Phys. Lett. 166B (1986) 468; Phys. Rev. D 34 (1986) 3286;
MAC collab., E. Fernandez et al., Phys. Rev. D 35 (1987) 1;
AMY collab., S. K. Kim et al., Phys. Lett. B223 (1989) 476;
TOPAZ collab., I. Adachi et al., Phys. Lett. B200 (1988) 391;
VENUS collab., K. Abe et al., J. Phys. Soc. Japan 56 (1987) 3767;
Z. Phys. C 45 (1989) 175.

[14] C. N. Yang, Phys. Rev. 77 (1950) 242.

[15] G. P. Lepage and S. J. Brodsky, Phys. Lett. 87B (1979) 359;
A. Duncan and A. H. Mueller, Phys. Rev. D 21 (1980) 1636;
E. W. N. Glover et al, Z Physics at LEP 1, CERN 89-08,
ed., G. Altarelli et al., Vol. 2 (1989) 1.

[16] OPAL collab., M. Z. Akrawy et al., Phys. Lett. B231 (1989) 530.

[17] F. E. Low, Phys. Rev. Lett. 14 (1965) 238;
A. Litke, Harvard Univ., Ph. D Thesis (1970) unpublished.

[18] ALEPH collab., D. Decamp et al., Phys. Lett. B236 (1990) 501;
OPAL collab., M. Z Akrawy et al., Phys. Lett. B244 (1990) 135;
L3 collab., B. Adeva et al., Phys. Lett. B247 (1990) 177.

[19] M. L. Laursen et al., Phys. Rev. D 23 (1981) 2795.

[20] F. M. Renard, Phys. Lett. 116B (1982) 269.

[21] F. Boudjema and F. M. Renard et al., Z Physics at LEP 1, CERN 89-08,
ed., G. Altarelli et al., Vol. 2 (1989) 185.

Tables

$\sqrt{s}$ (GeV)	$L_{\rm int}$ (pb^{-1})	$N_{\gamma\gamma}$	$\sigma_{\gamma\gamma}$ (pb)
88.23	0.586	20	39.5 ± 8.8
89.23	0.654	16	27.9 ± 7.0
90.24	0.373	11	33.5 ± 10.1
91.23	3.829	114	33.7 ± 3.2
92.22	0.501	10	22.4 ± 7.1
93.23	0.636	15	27.1 ± 7.0
94.23	0.631	19	35.0 ± 8.0
91.22	7.211	205	32.4 ± 2.3

Table 1: The centre of mass energies, $\sqrt{s}$, the integrated luminosities, $L_{\rm int}$, the numbers of events observed, $N_{\gamma\gamma}$, and the measured integrated lowest order cross sections, $\sigma_{\gamma\gamma}$, in the angular region $|\cos\theta| < 0.9$. Radiative corrections have been taken into account in the calculation. The errors on the cross section include both statistical and systematic ones, except for the systematic normalisation error on the luminosity measurement.

Experiment	$Br(Z^0 \to \gamma\gamma)$	$Br(Z^0 \to \pi^0\gamma)$	$Br(Z^0 \to \eta\gamma)$	$Br(Z^0 \to \gamma\gamma\gamma)$
OPAL (this experiment)	1.4×10^{-4}	1.4×10^{-4}	2.0×10^{-4}	6.6×10^{-5}
ALEPH		4.9×10^{-4}	4.6×10^{-4}	
DELPHI		3.0×10^{-4}	4.8×10^{-4}	
L3	2.9×10^{-4}	2.9×10^{-4}	4.1×10^{-4}	1.2×10^{-4}
OPAL [1]	3.7×10^{-4}	3.9×10^{-4}	5.8×10^{-4}	2.8×10^{-4}

Table 2: Comparison of upper limits on the branching ratios of $Z^0 \to \gamma\gamma$, $Z^0 \to \pi^0\gamma$, $Z^0 \to \eta\gamma$ and $Z^0 \to \gamma\gamma\gamma$. The limits were obtained at 95% confidence level. The data used in this paper include those used in our previous paper [1].

$\lvert\cos\theta\rvert$	$N_{\gamma\gamma}$	$\frac{d\sigma}{d\Omega}_{\gamma\gamma}$ (pb/str)
0.0-0.1	14	3.6 ± 1.0
0.1-0.2	9	2.5 ± 1.0
0.2-0.3	9	2.1 ± 0.8
0.3-0.4	18	4.6 ± 1.2
0.4-0.5	14	3.4 ± 1.0
0.5-0.6	18	5.2 ± 1.3
0.6-0.7	18	4.4 ± 1.1
0.7-0.8	40	10.3 ± 1.7
0.8-0.9	65	15.6 ± 2.0

Table 3: The $\lvert\cos\theta\rvert$ range, the numbers of events observed, $N_{\gamma\gamma}$, and the differential cross sections $\frac{d\sigma}{d\Omega}_{\gamma\gamma}$. Angular dependent radiative corrections have been taken into account in the calculation. The errors on the cross section include both statistical and systematic ones, except for the systematic normalisation error on the luminosity measurement.

Experiment	Λ_+ (GeV)	Λ_- (GeV)
OPAL (this experiment)	117	110
L3	103	118
OPAL [1]	82	89
AMY	65	
TOPAZ	94	59
VENUS	81	82
CELLO	84	44
JADE	66	75
MARK-J	72	
PLUTO	46	36
TASSO	61	56
HRS	59	59
MAC	66	67

Table 4: Comparison of lower limits on the cutoff parameters of the modified electron propagator $\Lambda_\pm$. The limits were obtained at 95% confidence level. The data used in this paper include those used in our previous paper [1].

$\sqrt{s}$ (GeV)	$L_{\rm int}$ ($\rm pb^{-1}$)	$N_{\gamma\gamma\gamma}^{obs}$	$N_{\gamma\gamma\gamma}^{exp}$
88.23	0.586	0	0.49
89.23	0.654	0	0.54
90.24	0.373	2	0.30
91.23	3.829	5	3.01
92.22	0.501	1	0.39
93.23	0.636	0	0.48
94.23	0.631	0	0.46
91.22	7.211	8	5.7

Table 5: The centre of mass energies, $\sqrt{s}$, the integrated luminosities, $L_{\rm int}$, the numbers of events observed, $N_{\gamma\gamma\gamma}^{obs}$, and the numbers of events expected, $N_{\gamma\gamma\gamma}^{exp}$. The background from $e^+e^- \rightarrow e^+e^-\gamma\gamma$ is included in the expectation.

Figure Captions

Figure 1: a) The distribution of the second largest electromagnetic cluster energy normalised to the beam energy (points with error bars), compared with the QED prediction for $e^+e^- \to \gamma\gamma$ (histogram). All the selection cuts but the cluster cut A1) have been applied. b) The distribution of the acollinearity angle of the two most energetic electromagnetic clusters (points with error bars), compared with the QED prediction for $e^+e^- \to \gamma\gamma$ (histogram). All selection cuts but the acollinearity angle cut A2) have been applied.

Figure 2: a) The measured integrated lowest order cross section for $e^+e^- \to \gamma\gamma$ (points with error bars), compared with the QED prediction (solid curve), within the polar angular range $|\cos\theta| < 0.9$. The average cross section is shown by a square with an error bar. The dashed curve shows the expectation with a Z^0 decay width of $\Gamma_{\gamma\gamma} = 0.36$ MeV (95% confidence level limit). b) The ratio of the measured differential cross section for $e^+e^- \to \gamma\gamma$ to the QED prediction (points with error bars). The solid curves show the expectations with the cutoff parameters Λ_+ =117 GeV and Λ_- =110 GeV (95% confidence level limits).

Figure 3: a) The ratio of the number of observed $e^+e^- \to \gamma\gamma\gamma$ events to the QED expectation. The dashed curve shows the expectations with a Z^0 decay width $\Gamma_{\gamma\gamma\gamma}$ =0.17 MeV (95% confidence level limit). b) The distribution of the invariant mass of the photon pairs normalised to $\sqrt{s}$ (points with error bars) compared to the QED expectation (histogram). There are three entries per event.

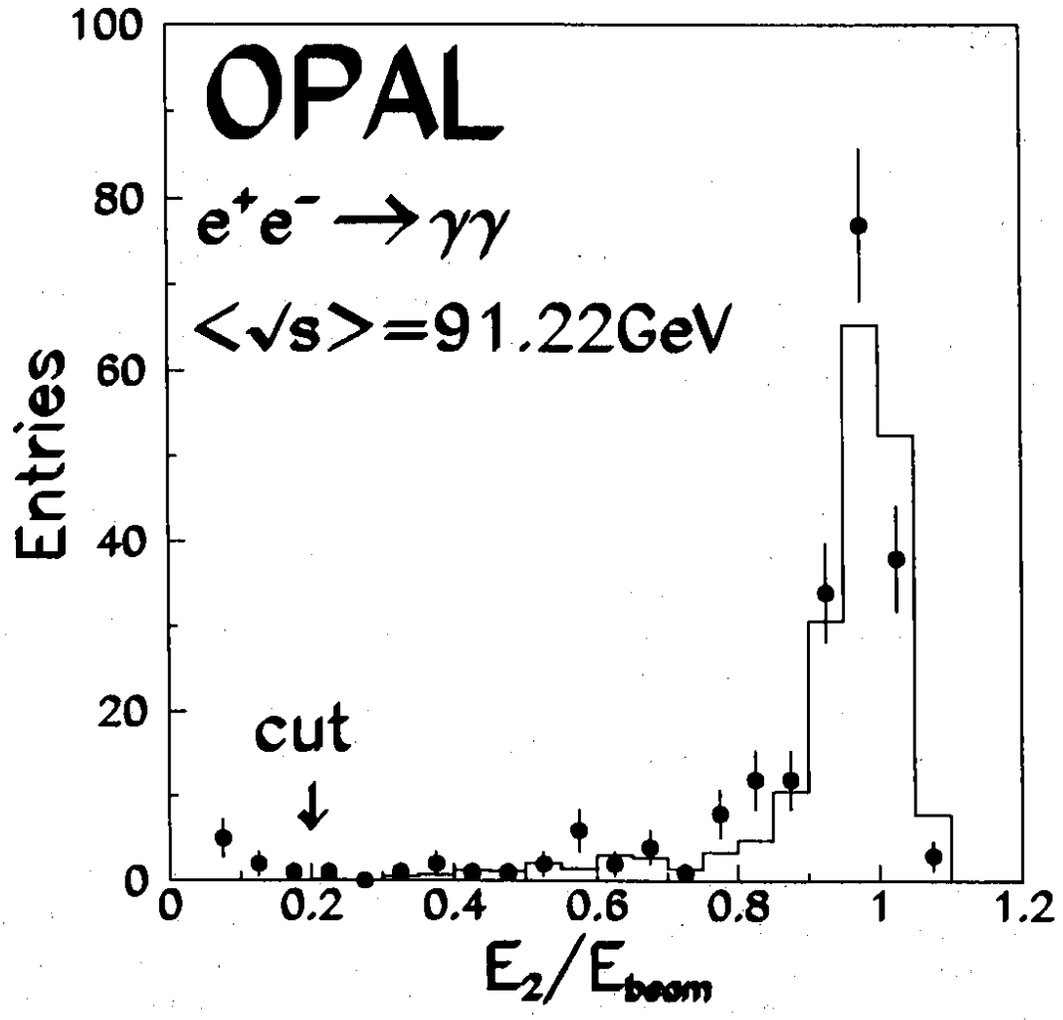
OPAL
$e^+e^- \rightarrow \gamma\gamma$
$\langle\sqrt{s}\rangle$=91.22GeV
Entries
cut
E_2/E_{beam}
0
20
40
60
80
100
0.2
0.4
0.6
0.8
1
1.2

figure 1a

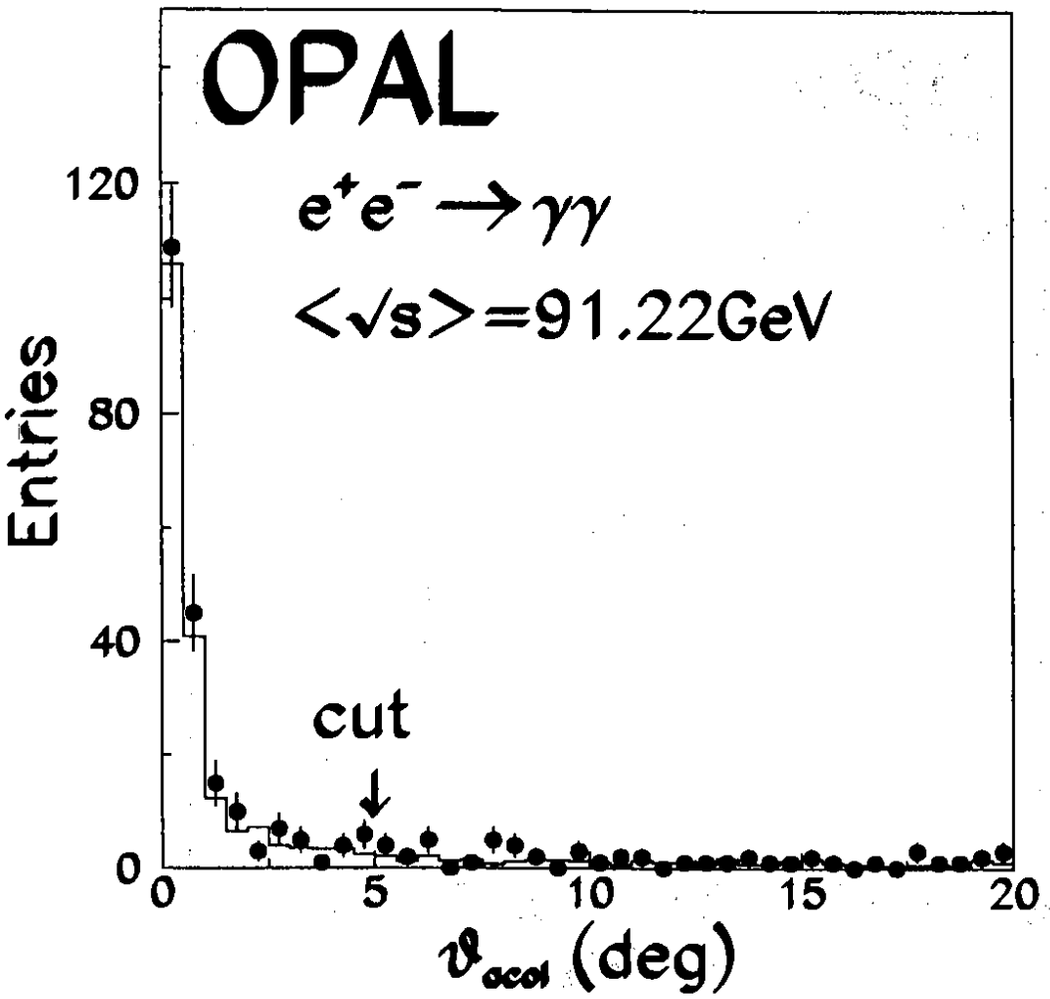
OPAL
$e^+e^- \rightarrow \gamma\gamma$
$\langle\sqrt{s}\rangle$=91.22GeV
Entries
120
80
40
0
cut
0
5
10
15
20
ϑ_{acol} (deg)

figure 1b

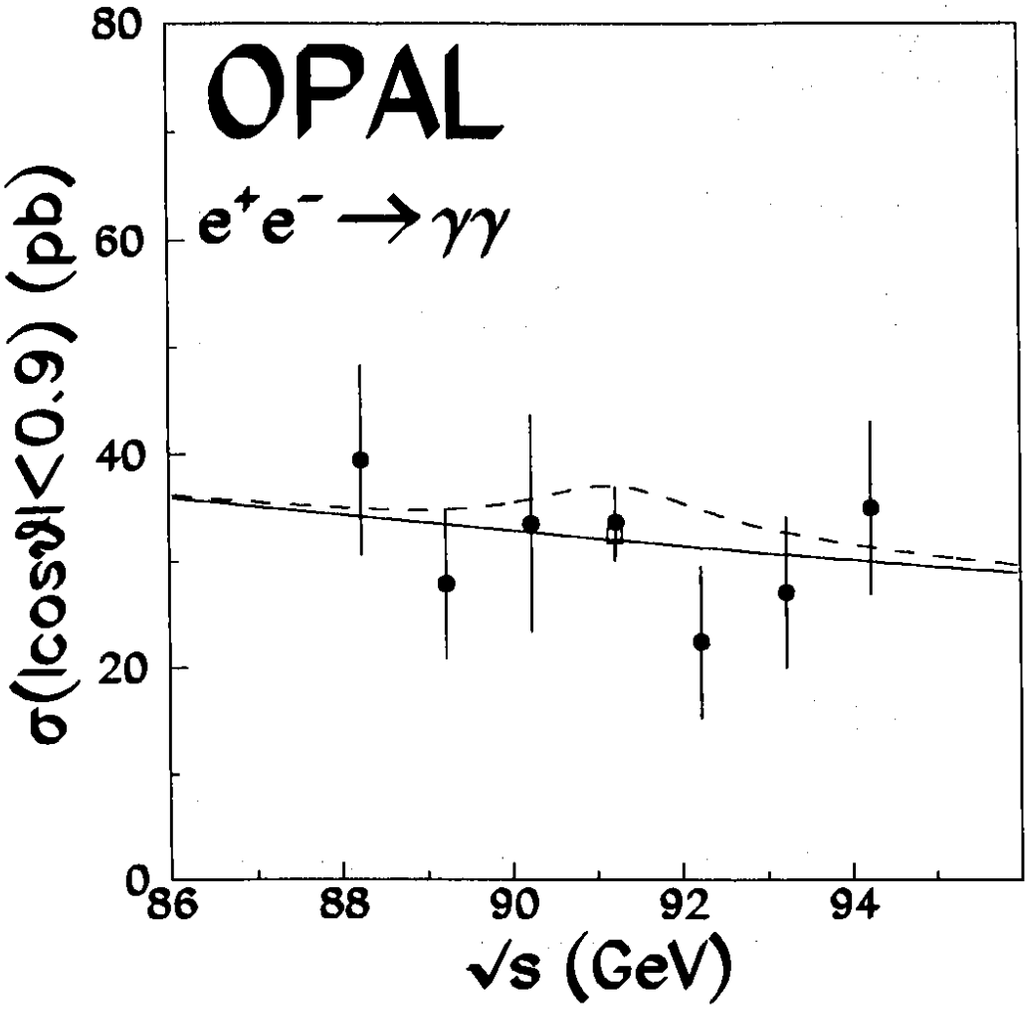
OPAL
$e^+e^- \rightarrow \gamma\gamma$
$\sigma(|\cos\vartheta|<0.9)$ (pb)
80
60
40
20
0
86
88
90
92
94
$\sqrt{s}$ (GeV)

figure 2a

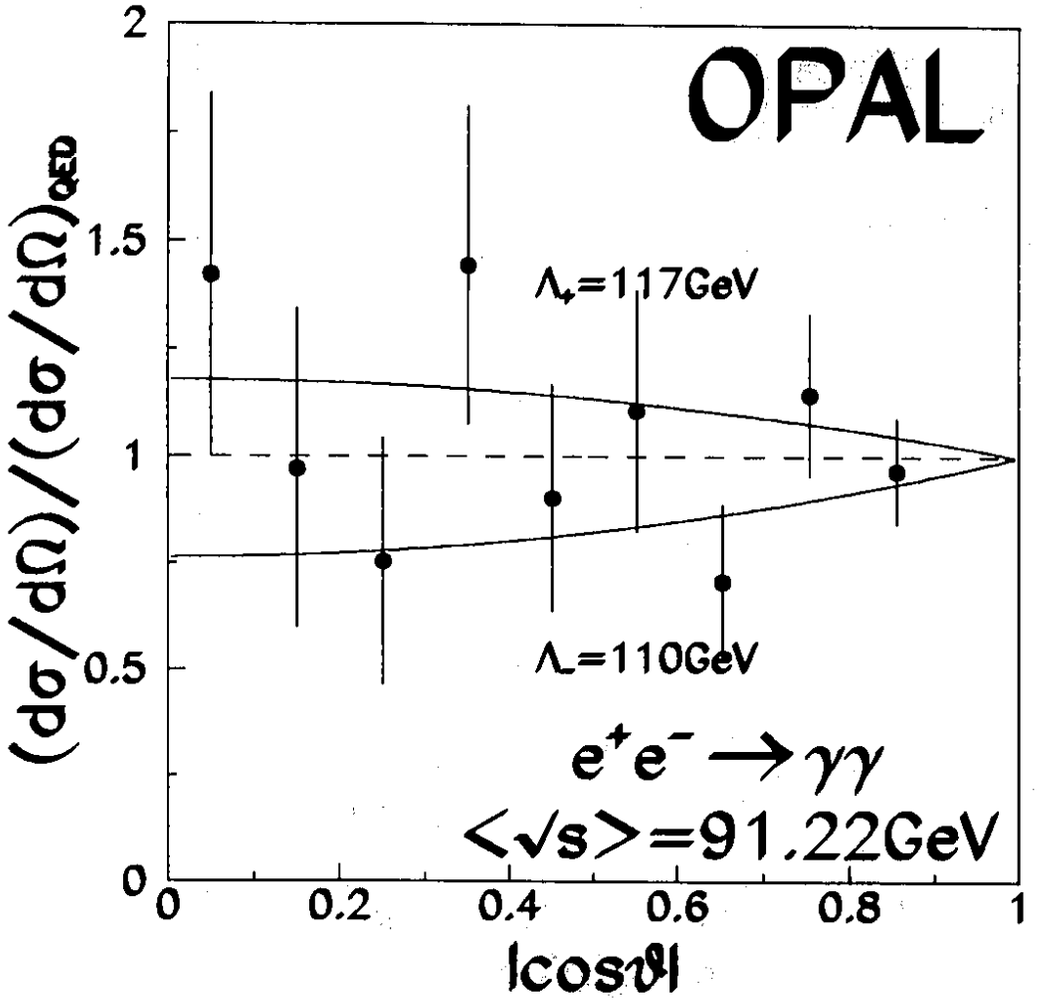
OPAL
Λ_+=117GeV
Λ_-=110GeV
$e^+e^- \rightarrow \gamma\gamma$
$<\sqrt{s}>$=91.22GeV
$(d\sigma/d\Omega)/(d\sigma/d\Omega)_{QED}$
$|\cos\vartheta|$
0
0.5
1
1.5
2
0.2
0.4
0.6
0.8

figure 2b

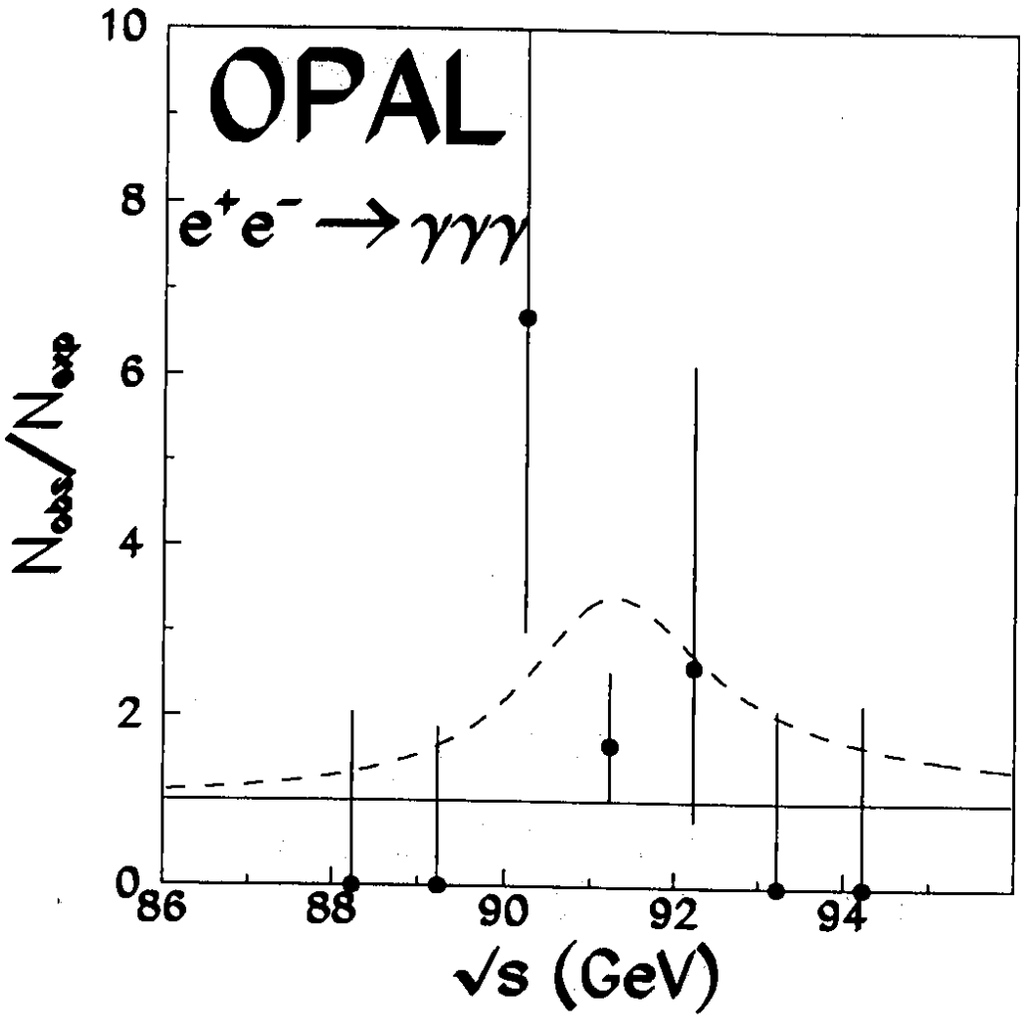
OPAL
$e^+e^- \rightarrow \gamma\gamma\gamma$
N_{obs}/N_{exp}
10
8
6
4
2
0
86
88
90
92
94
√s (GeV)

figure 3a

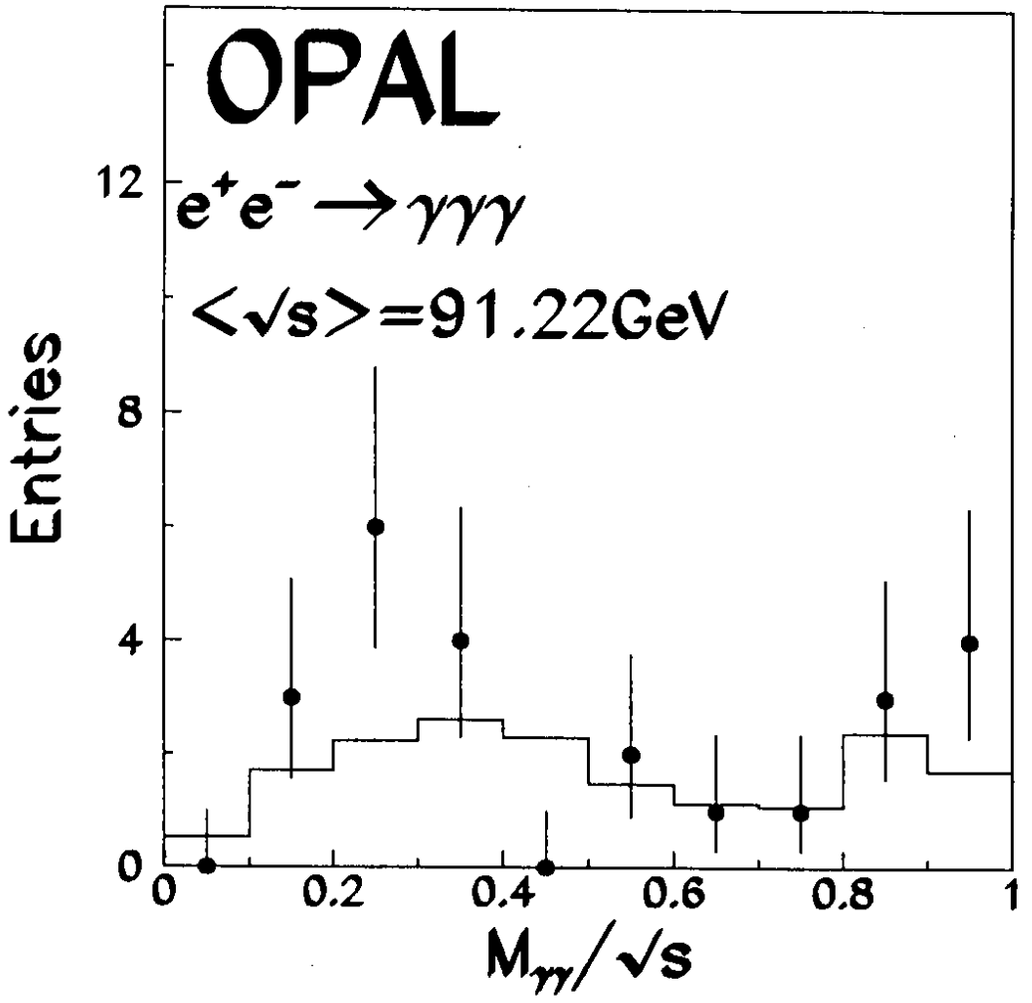

figure 3b

Imprimé au CERN. Prix : 0.70 Fr.